INTERACTION NOTES

Note 257

August 1975

INDUCED CURRENTS AND CHARGES ON THIN CYLINDERS IN A TIME-VARYING ELECTROMAGNETIC FIELD

Robert W. Burton
U. S. Naval Postgraduate School

and

R. W. P. King
Harvard University

ABSTRACT

The distributions of current and charge induced on the surface of electrically thin metal cylinders by an external electromagnetic field are described by means of theoretically and experimentally determined graphs. Various possible standing-wave patterns are shown including some with unexpected properties such as the coincidence of current and charge minima. A knowledge of these distributions is essential to the determination of the shielding properties of imperfectly conducting cylinders and cylinders with small apertures. It is also a prerequisite to an understanding of currents and charges on crossed metal cylinders including aircraft exposed to an electromagnetic pulse. The significance of the location of the junction in the standing-wave patterns is pointed out.

The experimental research was supported by the Joint Services Electronics Program at Harvard University under Contract N00014-67-A-298-0005.

1. Introduction

The distributions of current and charge that are induced on the conducting surfaces of missiles, aircraft, shielded transmission lines and other metal-clad bodies by an externally generated electromagnetic field in the form of a standing or traveling wave or pulse are of interest for several reasons. The most obvious is the determination of the scattered far field set up by them since it determines the radar cross section. No less important is a knowledge of the near field specifically in its relationship to the limited shielding properties of the metal skin when interrupted by small apertures [1],[2] or because it is imperfectly conducting [3]. Closely related and also involving the near field is the coupling between the exterior and the interior regions due to exposed conductors that pass through holes in the skin [4]. In all of these cases the field and possible currents on conductors in the interior are directly related to the currents and charges induced on the outside surfaces. Although the currents induced in circuits within a cylindrical sheath that simulates a missile and due to fields that penetrate the imperfectly conducting walls or enter through slots, holes or other apertures have been studied in some detail [1]-[4], the scope of the investigations has been limited to cylinders with radius a and half-length h that are electrically very thin ($a/\lambda << 1$) and relatively short ($h/\lambda \leq 1$). This range of study is clearly inadequate even to estimate results at frequencies for which the missile is electrically long or when the exciting field is a pulse containing a reasonably wide spectrum of frequencies. Investigations relating to the penetration of fields into crossed metal structures like airplanes are still in very early stages. Several studies using numerical methods have been made [5]-[8] to determine the distributions of current on electrically very thin crossed cylinders when the lengths of the

arms range between $h/\lambda = 0.1$ and 0.3. An analytical determination of the distributions of current and charge per unit length on mutually perpendicular crossed cylinders has been completed [9]. Theoretical descriptions and experimental verifications of such distributions are the subject of work in progress.

In order to obtain insight into the complicated phenomena involved when currents and charges are induced on metal structures by a periodic or transient electromagnetic field, it is advantageous to examine in greater detail than has heretofore been considered necessary the currents and charges induced on a straight electrically thin conductor when excited by an incident plane wave. Such a study can yield information that is useful not only for isolated cylinders but for crossed cylinders as well. Theory [9] and measurements have shown that the coupling between the currents in the arms of a crossed dipole involves the location of their junction in the standing-wave patterns of the currents and charges per unit length. Since these patterns are the result of a superposition of resonant and forced distributions, they are not entirely simple even along a single straight electrically thin cylinder with its axis parallel to the exciting field. This is shown in the following theoretical and measured results. A thorough understanding of their properties is a prerequisite to the investigation of the related but much more complicated problems encountered with crossed elements and electrically thick elements.

2. Theoretical Distributions of Current and Charge Per Unit Length Along Thin Cylinders Parallel to the Exciting Electric Field

The original interest in the current distribution along electrically thin conductors excited by an electromagnetic wave was in connection with their reradiating or scattering properties. In early work [10]-[12] approximate expressions for the distribution of current were derived or postulated as trial functions in variational methods specifically for calculating the back-scattering cross section. This is an average quantity not very sensitive to the detailed structure of the current. For the determination of the fields in small apertures much more accurate formulas are needed and these have been obtained for the currents in both shorter and longer thin wires in the ranges of half-lengths h given by $0 \leq h \leq 5\lambda/8$ [13] and $\lambda/4 < h < \infty$ [14], [15]. However, graphs of only a few lengths have been displayed and the complicated distributions arising from the superposition of resonant and forced induced currents have not been shown or discussed. The major purpose of this paper is to examine some of the principal standing-wave patterns for both the current and the charge per unit length in parasitic antennas and to verify these by direct measurement.

A complete study of the several interesting and important distributions of current and charge per unit length is possible only if wires up to at least several wavelengths long are included. For this reason computations have been carried out with the formulas for currents and charges per unit length in relatively long antennas as given by Chen and Wu [14, eqs. 10.152 and 10.153]. When the electric field is normally incident and parallel to the axis of the antenna, the normalized current I(z) and charge per unit length q(z) are given by:

$$\frac{I(z)}{E_z^{inc}{}_\lambda} = \frac{i}{4\pi^2\zeta_0}\left\{\frac{4\pi^2}{\Omega_1} - \frac{i2\pi}{k}[M(h+z) + M(h-z)] + \frac{C_s}{2}[U(h+z) + U(h-z)]\right.$$
$$\left. \times \cos kz + C_s[S(h+z) - S(h-z)]\sin kz\right\} \quad (1)$$

$$\frac{q(z)}{E_z^{inc}{}_\lambda} = -\frac{\varepsilon_0}{8\pi^3}\left\{\frac{2\pi}{k}[1 + C_s\cos kh][M(h-z) + M(h+z)] + \frac{C_s}{2}[S(h+z)\right.$$
$$\left. - S(h-z)]\cos kz + \frac{C_s}{2}[U(h+z) + U(h-z)]\sin kz\right\} \quad (2)$$

where

$$C_s \doteq -\frac{4\pi^2/\Omega_1 - (i2\pi/k)M(2h)}{T(2h)\cos kh + S(2h)\sin kh} \quad (3)$$

$$\Omega_1 = \Omega_0 + i\pi/2 \quad ; \quad \Omega_0 = \ell n(2/ka) - 0.5772 \quad (4)$$

$$M(X) = \frac{i2}{X}e^{ikX}\left[\frac{1}{\Omega_2(X)} - \frac{1}{\Omega_3(X)}\right] \quad (5)$$

$$\Omega_2(X) = 2[\ell n(1/ka) - 0.5772] + \ell n(2kX) + 0.5772 - i\pi/2 \quad (6)$$

$$\Omega_3(X) = \Omega_2(X) + 2\pi \quad (7)$$

$$\left.\begin{matrix} S(X)/2\pi \\ T(X)/2\pi i \end{matrix}\right\} = -\ell n[1 + i\pi(\Omega_0 - \ell n\ 2)^{-1}] - (\pi^2/12)[(\Omega_0 - 2\ \ell n\ 2)^{-2}$$
$$- (\Omega_0 - 2\ \ell n\ 2 + i\pi)^{-2}] \pm \ell n[\Omega_3(X)/\Omega_2(X)] + 0.825[\Omega_2^{-2}(X)$$
$$- \Omega_3^{-2}(X)] - M(X)/4k \quad (9)$$

$$-U(X)/4\pi i = \ell n[\Omega_3(X)/\Omega_2(X)] + 0.825[\Omega_2^{-2}(X) - \Omega_3^{-2}(X)] + M(X)/4k \quad (10)$$

These formulas were derived with the time dependence $e^{-i\omega t}$; they can be converted to $e^{j\omega t}$ with the substitution $i = -j$. The formulas (1) and (2) are not good approximations within distances of a quarter wavelength or less of

the ends of the wire where, however, the current is known to vanish so that simple extrapolation is possible. Their derivation assumes that $ka << 1$ and $kh > \pi/2$. The approximation improves as the length of the wire is increased. The theoretical distributions of current $I(z)$ and charge per unit length $q(z)$ shown in the several graphs to be discussed were computed from (1) and (2). Magnitudes and phases are shown in all cases but a better understanding of these is obtained from the graphs for the real and imaginary parts, i.e., the components in phase and in phase quadrature with the active electric field along the axis.

3. Measurement of Distributions of Current and Charge Per Unit Length

An apparatus was constructed for measuring currents and charges per unit length along a smooth monopole erected vertically on a large metal ground plane. The parasitic monopole consisted of a slotted brass tube with a flat end cap erected vertically on a large aluminum ground screen. It was illuminated by a vertically polarized electromagnetic field generated by a long driven antenna with a corner reflector nearly ten wavelengths away so that the phase fronts of the incident waves at the parasitic antenna approximated a plane as assumed in the theory. Measurements were made at two frequencies for which the electrical radii of the antenna were $ka = 0.033$ and $ka = 0.044$. Thus, the antenna was actually not electrically very thin. In particular, the theoretical expansion parameter $\Omega_0 = \ell n(2/ka) - 0.577$ has the values 3.52 and 3.23. These are apparently not large enough to expect great quantitative accuracy from the theory. However, as shown by Kao [16] in his study of currents on electrically thick cylinders, the axial distribution of current when the incident electric field is parallel to the axis is not sensitive to the radius even when its transverse distributions departs somewhat from rotational

symmetry and significant transverse currents occur near the ends. It is, therefore, not surprising and is reassuring to find that distributions of current and charge per unit length computed from (1) and (2) with ka = 0.04 (for which $\Omega_0 = 3.33$) do not differ greatly from those computed with ka = 0.12 (for which $\Omega_0 = 2.24$) as shown in several of the theoretical graphs. It may be concluded that for qualitative and approximate quantitative purposes the theoretical results are entirely adequate. In particular, they are invaluable in providing the means to clarify the peculiarities and intricacies observed in the measured distributions.

The instrumentation consisted of a flush-mounted monopole for a charge probe and a small shielded loop as a current probe. These could be moved along a slot in the antenna by an internal mechanism controlled by a rack-and-pinion positioner mounted beneath the ground plane. In order to obtain different standing-wave patterns, the length of the antenna was varied over a wide range. However, measurements of current and charge were not made over the full length - only over a distance of approximately $3\lambda/4$ measured from the ground plane. It will be seen that this is adequate to confirm the theoretical distributions computed for much longer antennas.

4. Description of Theoretical and Experimental Standing-Wave Patterns

The first monopole investigated was $3\lambda/4$ long - a length near resonance. The theoretical distributions of current and charge per unit length are shown in Fig. 1. Both amplitudes and phases resemble those along a resonant open-ended section of coaxial line in that the maxima of the current and the minima of the charge are virtually coincident near $kz = 0$ and π or at $\lambda/4$ and $3\lambda/4$ from the open end. Correspondingly, the minima of the current and maxima of the charge occur close together at $kz = \pi/2$ and at the open end $kz = kh = 3\pi/2$. Rapid changes in phase by 180° occur near the minima, indicating a reversal in direction of the principal components of both current and charge. While the amplitude and phase of the charge behave very closely like those in a coaxial line with an open end, there are significant differences in the distribution of current. These include a minimum that is not as sharp and deep, two maxima that differ greatly from each other in amplitude - the one at $kz = 0$ is much smaller, and a phase angle θ_I that changes only gradually through the 180°. These differences are a consequence of the continuous uniform excitation along the entire length instead of by a single localized generator. Measured curves for the same electrical length but with a slightly smaller value of ka are shown in Fig. 2. All four curves are seen to agree well in all significant details with the corresponding theoretical ones.

The theoretical distributions of current and charge for a monopole with $h = \lambda$ are shown in Fig. 3. Note that the maximum of current and the minimum of charge at $kz = \pi$ have remained just as with $h = 3\lambda/4$ in Fig. 1. However, the minimum of current at $kz = \pi/2$ has now disappeared even though the maximum of charge has remained. The zero of charge at $kz = 0$ is now associated with a minimum instead of a maximum of current as in Fig. 1. Similarly the zero of current at the end ($z = h$) is now associated with a minimum of charge

instead of a maximum as in Fig. 1. The phase angle θ_q of the charge behaves just as in Fig. 1: a rapid change through 180° occurs at the minimum of charge. The phase angle θ_I of the current, on the other hand, differs dramatically from that in Fig. 1. There is no 180° phase change; indeed the phase is remarkably constant with a maximum change of less than 90° over the entire wavelength. Measured curves corresponding to the theoretical ones in Fig. 3 are shown in Fig. 4. Again they are in substantial general agreement with the theoretical ones. The effect of changing ka from 0.04 to 0.12 is also shown in Fig. 3.

When the length of the monopole is increased to $3\lambda/2$ as shown in Fig. 5, the distribution of charge remains conventional in both amplitude and phase. Maxima occur at intervals of $\lambda/2$; and these are displaced by $\lambda/4$ from the minima. The phase angle θ_q changes rapidly by 180° at the minima. The distribution of current is quite different. Its maxima occur at intervals of λ, as do its minima. The phase angle θ_I is sensibly constant over the entire length of the antenna with only relatively small (compared with variations in θ_q) dips at the minima of current.

The measured curves for $h = 3\lambda/2$ are shown in Fig. 6. As indicated previously, measurements were made only out a distance $kz = 3\pi/2$ from the ground plane. A comparison of Figs. 5 and 6 shows that the theoretical and measured magnitudes $|q(z)|$ and phase angles θ_q of the charge per unit length agree well as do the phase angles θ_I of the currents. However, whereas the theoretical current amplitude has a minimum at $kz = \pi$, the measured curve shows a peculiar minor maximum. This is not an error but is readily explained with the help of a slight increase in the length of the antenna for the theoretical calculation. Fig. 7 shows the same theoretical curves but for $kh = 10.2$ instead of $kz = 3\pi$. The amplitude and phase angle of the charge and the

phase angle of the current show little change. But, a minor maximum now occurs at $kz = \pi$ in the graph for $|I(z)|$ in close correspondence with the measured curve in Fig. 6. Actually, this minor maximum is considerably greater than the measured one, indicating that an even smaller increase in length would have sufficed. Thus, it is seen that the standing-wave pattern of current can be very sensitive to the length of the antenna.

The final example of the distributions of current and charge per unit length is for a near resonant length with $h = 5\lambda/4$ - a half-wavelength longer in half-length than used in Fig. 1. In this case the charge distribution once again looks conventional with maxima at intervals of a half-wavelength and 180° changes in the phase angle as the amplitude goes through a minimum. A zero of charge per unit length is at the ground plane, a maximum at the open end. The current has maxima at the minima of charge, but whereas the maxima at $kz = 0$ and $kz = 2\pi$ are almost equal in magnitude and quite large, that at $kz = \pi$ is much smaller. Furthermore, the phase angle θ_I has equal values near $kz = 0$ and $kz = 2\pi$, but quite a different range of values near $kz = \pi$. Measured curves for an antenna of length $kh = 5\pi/2$ are shown in Fig. 9. The theoretical and measured distributions of both amplitudes and phase angles are very much alike.

A study of the several distribution curves in Figs. 1 through 9 shows that the charge per unit length behaves in a very simple and predictable manner. In a zero-order approximation it is given by

$$q(z) \sim \sin kz \tag{11}$$

At the base of a monopole or the center of a dipole the charge per unit length must vanish to satisfy the symmetry condition $q(-z) = -q(z)$. All of

the graphs of q(z) are quite well approximated by the simple form (11) except for the occurrence of deep minima instead of nulls. These must be accounted for by higher-order terms.

In order to understand the peculiarities in the standing-wave patterns of the current, it is advantageous to examine the behavior of the components of the induced current that are in phase and in phase quadrature with the incident electric field. A set of graphs of $|I(z)|$ and θ_I and also of the in-phase component $I_R(z)$ and the quadrature component $I_I(z)$ for five lengths ranging from $kh = 9\pi/4$ to $kh = 11\pi/4$ with the near resonant length $kh = 5\pi/2$ at the center are shown in Fig. 10. It is seen in all of these that the curves for the real and imaginary parts of the current are much simpler than those for the magnitude and the phase angle. Except near the end at $z = h$ their leading terms can be approximated by shifted cosines of the type

$$I_R(z) \doteq A_R + B_R \cos kz \quad , \quad I_I(z) \doteq A_I + B_I \cos kz \tag{12}$$

where the A's and B's are real constants that depend on the length of the antenna in no simple manner [9]. It is readily seen by a comparison of the several sets of graphs how the different combinations of $I_R(z)$ and $I_I(z)$ shown in Fig. 10 combine to give the complicated-looking quite different curves for $|I(z)|$ and θ_I.

5. Standing Waves for Arbitrary Incidence

When the normal to the plane wave front of the incident wave makes an angle θ with the axis of the antenna instead of 90° as at normal incidence, the determination of the distribution of current is complicated by the fact that $I(-z) \neq I(z)$. A complete analysis of this problem has been carried out for short and moderately long antennas by King [13] and for long antennas by

Chen [15]. The standing-wave patterns along an isolated parasitic antenna with the electrical full length $2kh = 8\pi$ as determined by Chen [15] are shown in Fig. 11 for five angles of incidence. The graph for normal incidence, $\theta = 90°$, is the simple shifted cosine distribution, $|I(z)| \sim 1 - \cos kz$. Even a very small departure from normal incidence has a significant effect as shown by a comparison of the graph for $\theta = 88°$ with that for $\theta = 90°$. As the angle of incidence departs more and more from $\theta = 90°$, the standing-wave pattern changes greatly as seen from the graphs for $\theta = 60°$, 45° and 30°. Note that when $\theta = 30°$, current maxima occur at the normal intervals of a half-wavelength for resonance, whereas at $\theta = 90°$ they occur at the antiresonant intervals of a full wavelength.

The strong dependence of the distribution of current on a long parasitic antenna on small changes in the angle of incidence suggests a similar sensitivity to small departures of the incident wave front from the ideal plane surface due to curvature. Some of the small differences between the theoretical and measured curves may be a consequence of the fact that the transmitting antenna was at a large but finite distance from the parasitic element, so that the incident wave front was a large sphere, not a plane.

6. Significance of Standing-Wave Patterns for Crossed Dipoles

A principal reason for examining in detail the standing-wave patterns of the induced current and charge per unit length along a conductor with the electric field parallel to its axis is to establish a physical basis of understanding for the much more complicated distributions which obtain when a second conductor is connected across the first. The critical and independent aspects of this problem arise specifically when the two elements are mutually perpendicular and one of them is parallel to the active electric field. With

this configuration the axial currents and associated charges in the element perpendicular to the electric field are induced entirely by capacitive coupling to the charges in the element parallel to the field. This coupling is determined primarily by the conditions of charge at and near the junction, but also by forces acting among all charges at all points along the two conductors.

An examination of the distributions of current and charge per unit length in Figs. 1 through 10 reveals a number of possible special conditions at a junction. Thus in Figs. 1 and 2, a transverse conductor could be located at $kz = \pi$ where the current has a maximum, the charge per unit length a minimum; or it could be placed at $kz = \pi/2$ where the reverse is true: the charge per unit length has a maximum, the current a minimum. A transverse conductor located at $kz = \pi$ along the antenna with the distributions shown in Figs. 3 and 4 would also be located at a maximum of current and minimum of charge as for Fig. 1. However, the conditions at $kz = \pi/2$ are quite different: there is a maximum of charge here but no minimum of current. Note that in Fig. 3 the minima of current occur with the minima (not the maxima) of charge at $z = 0$ and $z = h$. Fig. 5 presents yet another set of conditions. A cross arm placed at $kz = \pi$ is at a minimum of charge per unit length just as in Figs. 1 and 3, but it is simultaneously at a minimum of current, not a maximum as in Figs. 1 and 3. On the other hand, only a half-wavelength away at $kz = 2\pi$, it would be at a minimum of charge and a maximum of current. An examination of Figs. 7 and 9 shows a further variety of conditions at possible junction points for a cross arm.

When a transverse conductor is placed at locations of maximum charge and minimum current, or minimum charge and maximum current, or minimum charge and minimum current, or at some intermediate point in the standing-wave pattern

along an antenna in an electric field, the forces acting to induce currents in it differ greatly. Evidently the standing-wave patterns on the four arms of a crossed dipole depend not only on their individual lengths but also on the relative location of the junction point. The complete interaction of the currents and charges in crossed dipoles is the subject of work in progress.

7. Conclusion

The standing-wave patterns of the distributions of current and charge per unit length along an electrically thin conductor illuminated by a linearly polarized periodic electric field have been studied in detail. Graphs of a variety of quite different patterns are shown based on theoretical and experimental data - these are in good agreement. The results are significant directly for determining the steady-state or transient fields that penetrate to the interior of a rocket, missile, or other metallically shielded cylinder through the imperfectly conducting skin or small cracks or apertures in it. They provide an important background of information and understanding for the study of crossed metal structures, specifically the electrically thin crossed dipole. Finally, they serve as an indication of the general disposition of axially distributed currents and charges on the surfaces of structures that are not electrically thin but long compared with their maximum cross-sectional dimension. They throw no light on distributions of transverse currents or on the interaction between axial and transverse currents in this more general problem. Measurements on electrically thick structures are planned.

References

[1] C. D. Taylor and C. W. Harrison, Jr., "On the excitation of a coaxial line through a small aperture in the outer sheath," Interaction Note 104, Jan 1972.

[2] C. W. Harrison, Jr. and R. W. P. King, "Excitation of a coaxial line by the propagation of an electromagnetic field through a transverse slot in the sheath, Interaction Note 87, Oct 1971.

[3] R. W. P. King and C. W. Harrison, Jr., "Cylindrical shields," Interaction Note 30, March 1961.

[4] R. W. P. King and C. W. Harrison, Jr., "Transmission line coupled to a cylinder in an incident field," Interaction Note 72, May 1971.

[5] C. D. Taylor, "Electromagnetic scattering from arbitrary configurations of wires," IEEE Trans. Antennas Propagat., Vol. AP-17, pp. 662-663, Sept. 1969.

[6] C. D. Taylor, S.-M. Lin and H. V. McAdams, "Scattering from crossed wires," IEEE Trans. Antennas Propagat., Vol. AP-18, pp. 133-136, Jan. 1970.

[7] C. M. Butler, "Currents induced on a pair of skew-crossed wires," IEEE Trans. Antennas Propagat., Vol. AP-20, pp. 731-736, Nov. 1972.

[8] H. H. Chao and B. J. Strait, "Radiation and scattering by a configuration of bent wires with junctions," IEEE Trans. Antennas Propagat., Vol, AP-19, pp. 701-702, Sept. 1971.

[9] R. W. P. King and T. T. Wu, "Analysis of crossed wires in a plane-wave field," Interaction Note 216, July 1974.

[10] J. H. Van Vleck, F. Block and M. Hamermesh, "Theory of radar reflection from wires and thin metallic strips," J. Appl. Phys., Vol. 18, pp. 274-294, March 1947.

[11] C. T. Tai, "Electromagnetic back-scattering from cylindrical wires," J. Appl. Phys., Vol. 23, pp. 909-916, 1952.

[12] R. W. P. King, Theory of Linear Antennas. Cambridge, Mass.: Harvard University Press, 1956, pp. 503-511.

[13] R. W. P. King, "Current distribution in arbitrarily oriented receiving and scattering antenna," IEEE Trans. Antennas Propagat., Vol. AP-20, pp. 152-159, March 1972.

[14] C.-L. Chen and T. T. Wu, pp. 446-454 in Antenna Theory, Part I, R. E. Collin and F. J. Zucker, Eds. New York: McGraw-Hill, 1969.

[15] C.-L. Chen, "On the scattering of electromagnetic waves from a long wire," Radio Science, Vol. 3(N.S.), pp. 585-598, June 1968.

[16] C. C. Kao, "Three-dimensional electromagnetic scattering from a circular tube of finite length," J. Appl. Phys., Vol. 40, pp. 4732-4740, 1969.

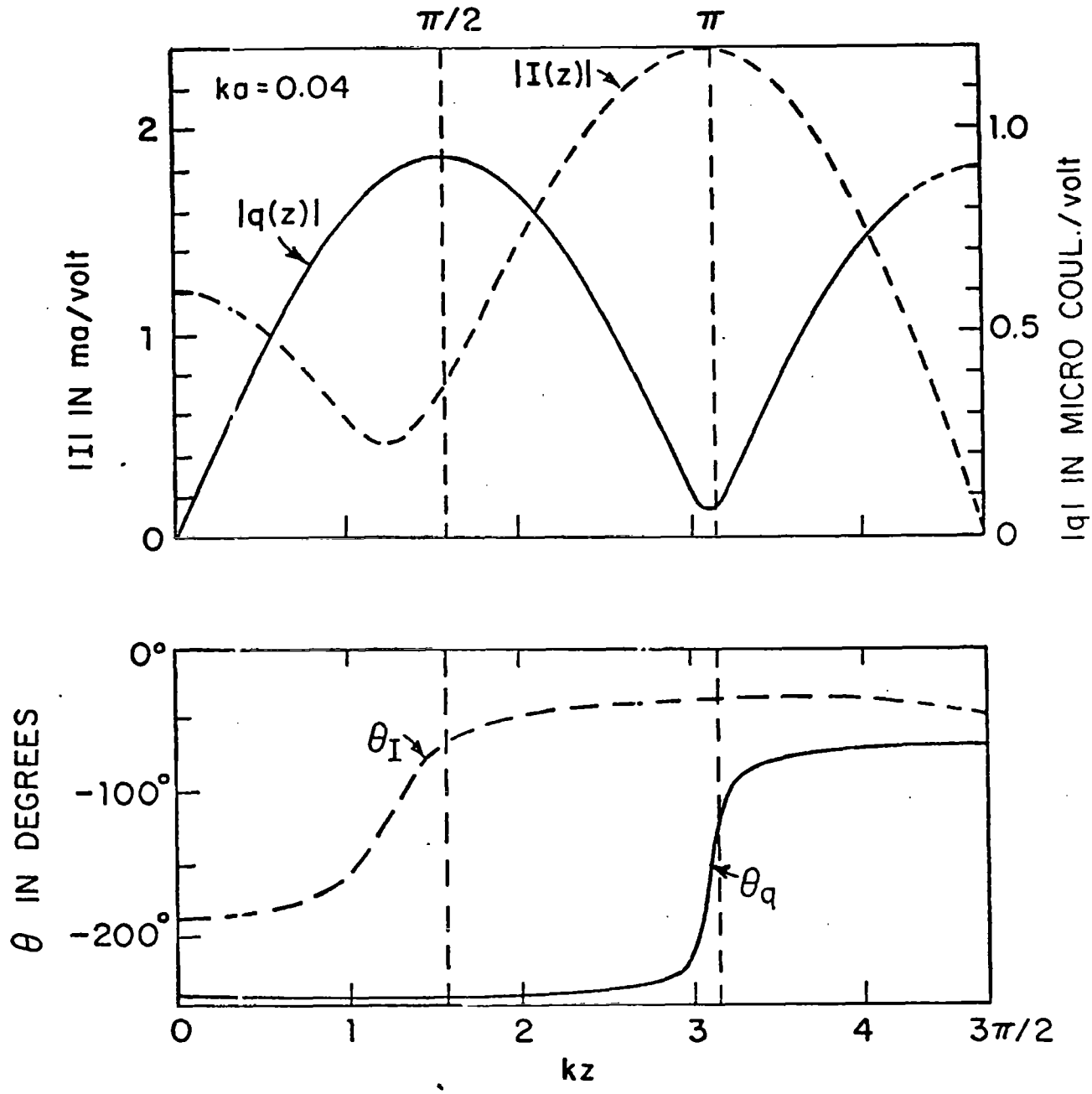

FIG. 1 THEORETICAL DISTRIBUTIONS OF CURRENT AND CHARGE IN PARASITIC MONOPOLE IN NORMALLY INCIDENT FIELD; $h = 3\lambda/4$.

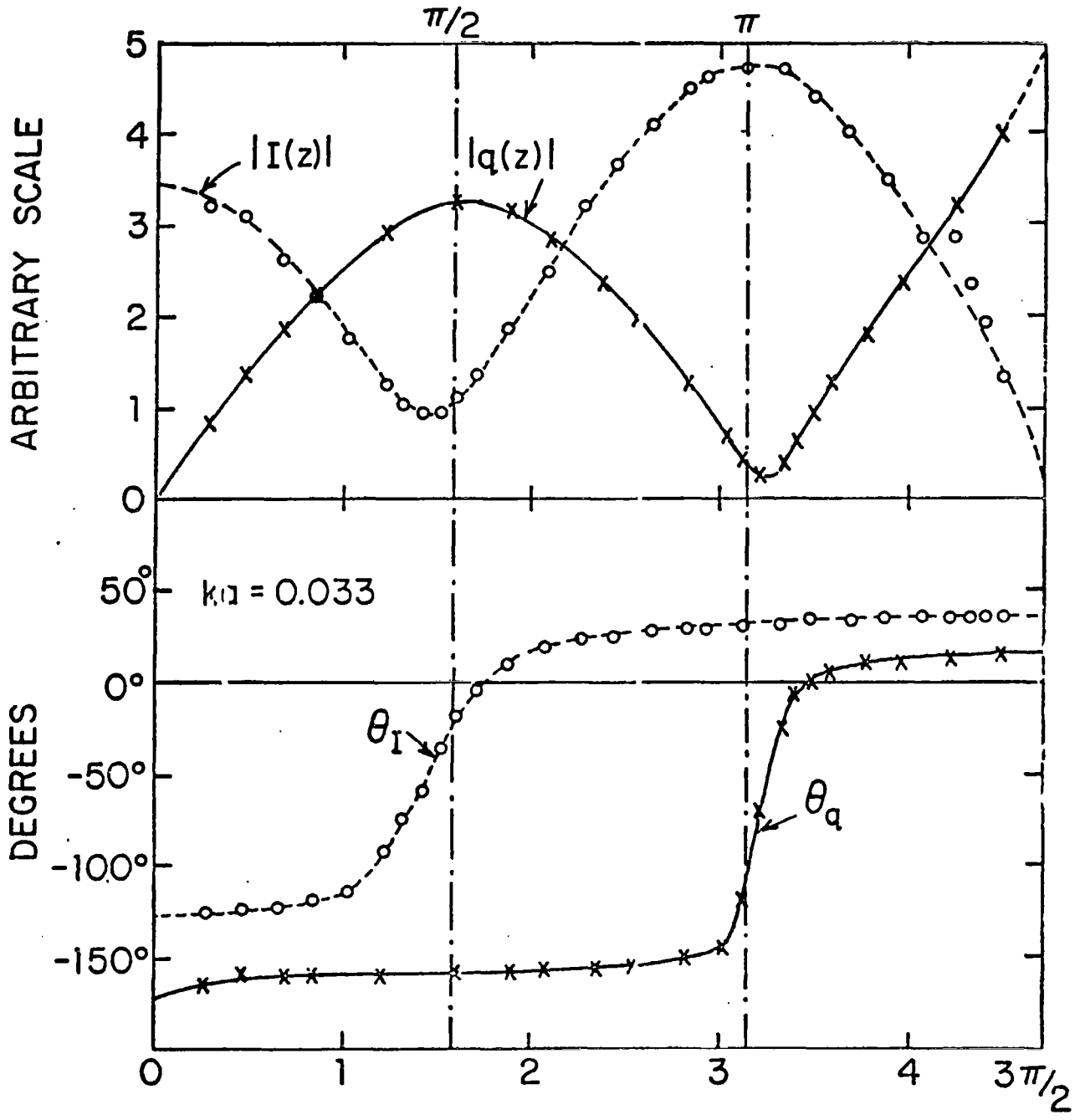

FIG. 2 MEASURED DISTRIBUTIONS OF CURRENT AND CHARGE IN PARASITIC MONOPOLE IN NORMALLY INCIDENT FIELD, $h = 3\lambda/4$

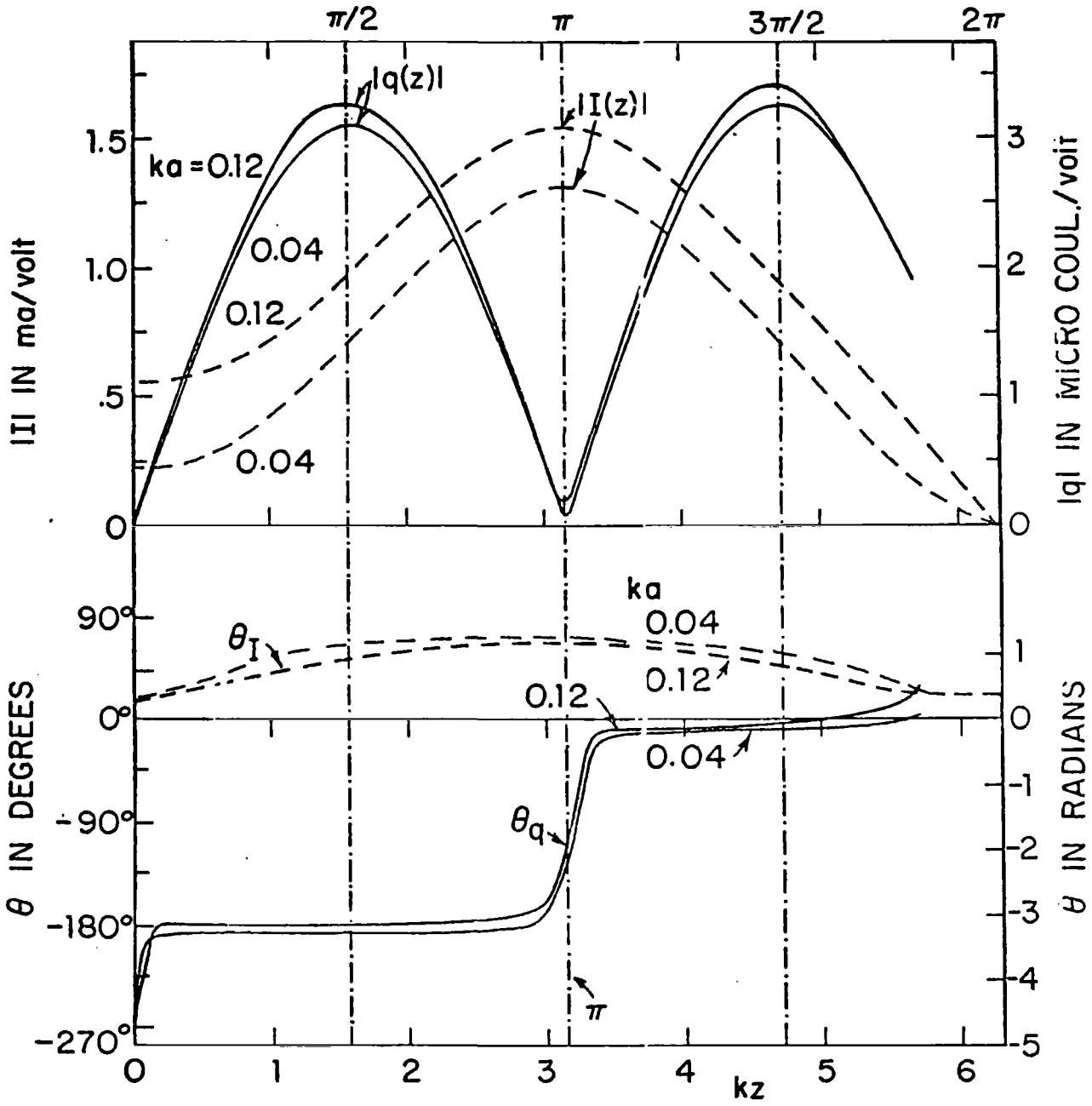

FIG. 3 THEORETICAL DISTRIBUTION OF CURRENT AND CHARGE IN PARASITIC MONOPOLE IN NORMALLY INCIDENT FIELD $h = \lambda$

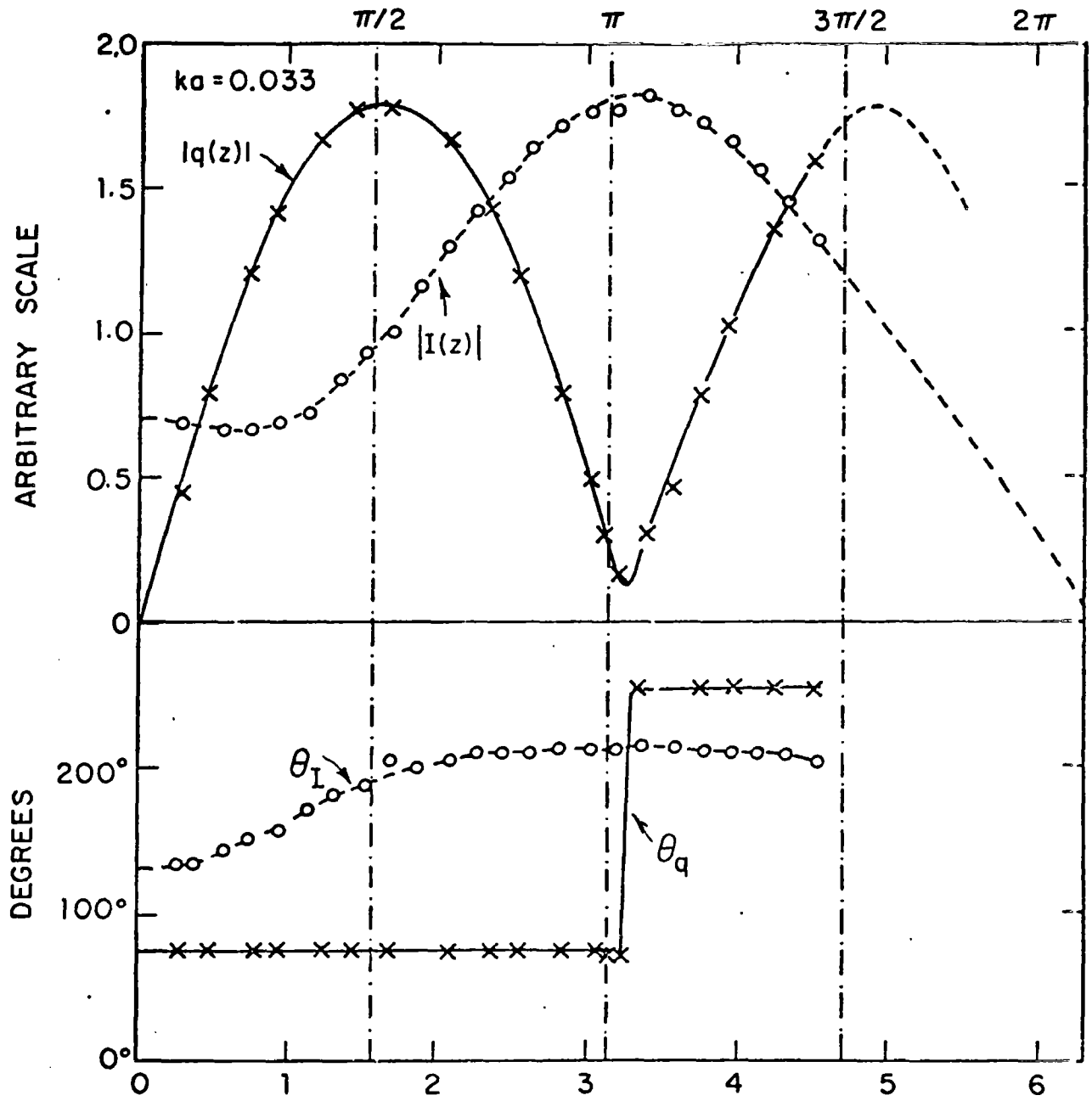

FIG. 4 MEASURED DISTRIBUTION OF CURRENT AND CHARGE IN PARASITIC MONOPOLE IN NORMALLY INCIDENT FIELD, $h = \lambda$.

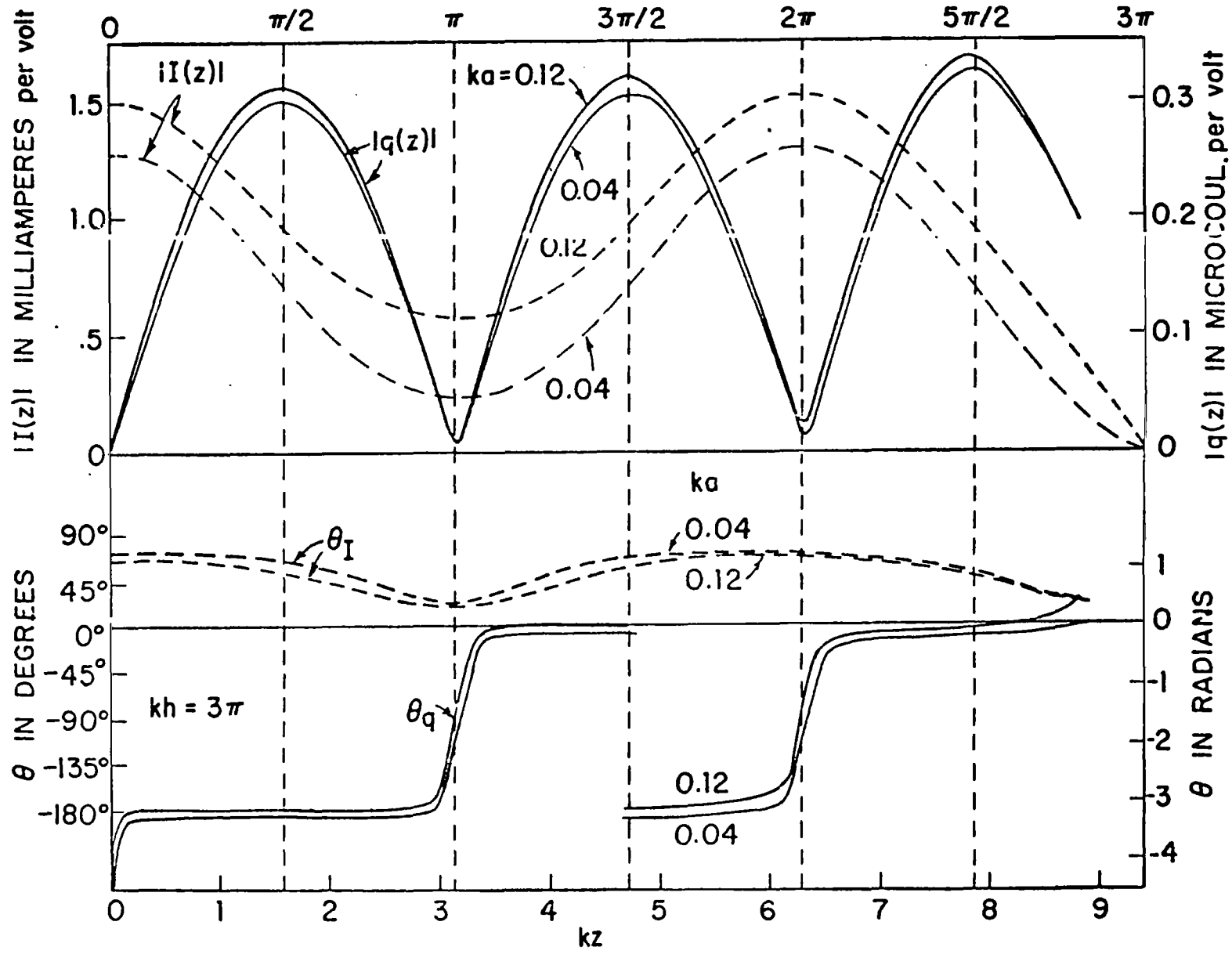

FIG. 5 THEORETICAL DISTRIBUTIONS OF CURRENT AND CHARGE IN PARASITIC ANTENNA IN NORMALLY INCIDENT FIELD, h = 1.5 λ

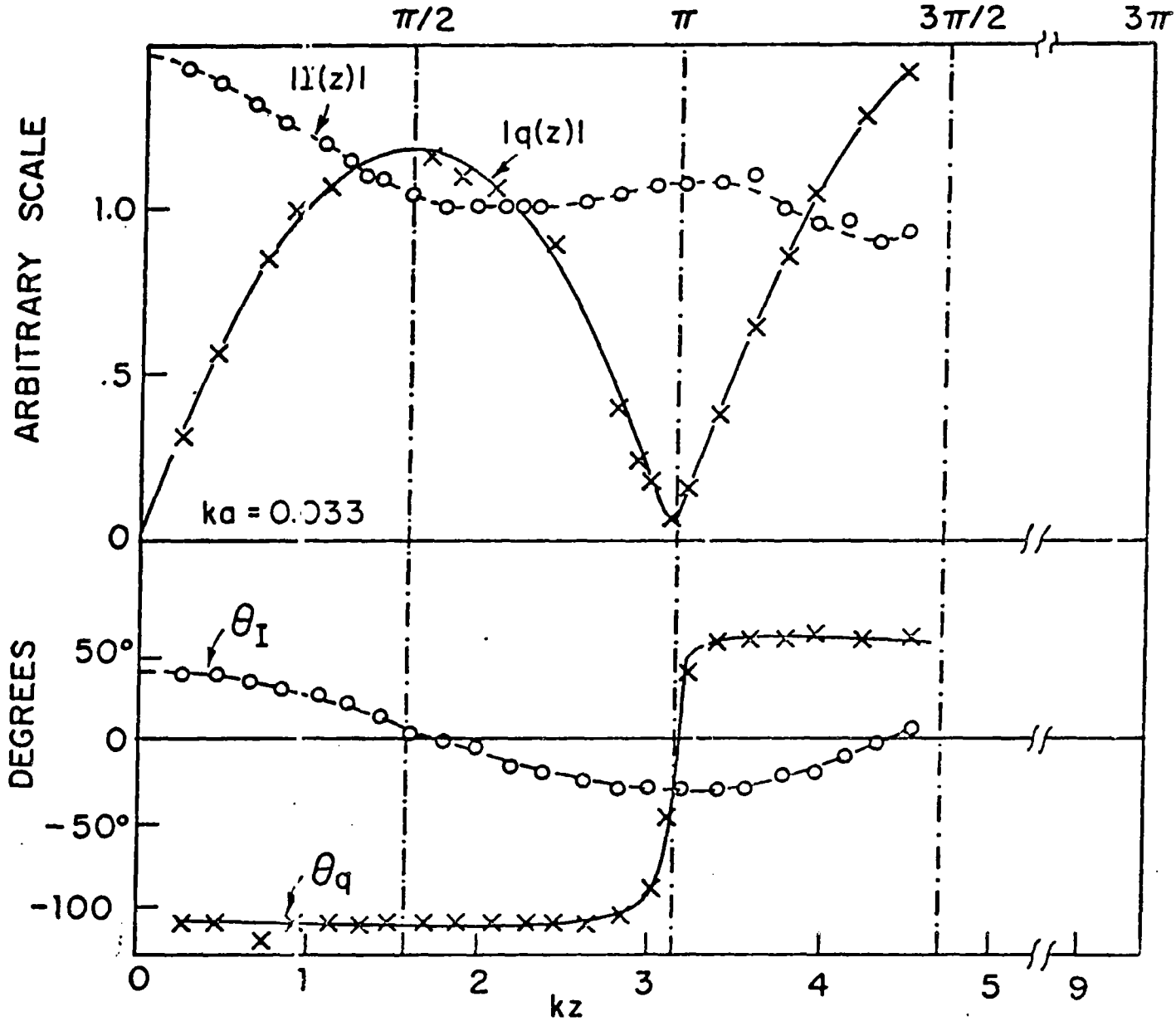

FIG. 6 MEASURED DISTRIBUTIONS OF CURRENT AND CHARGE IN PARASITIC MONOPOLE IN NORMALLY INCIDENT FIELD. $h = 1.5\lambda$.

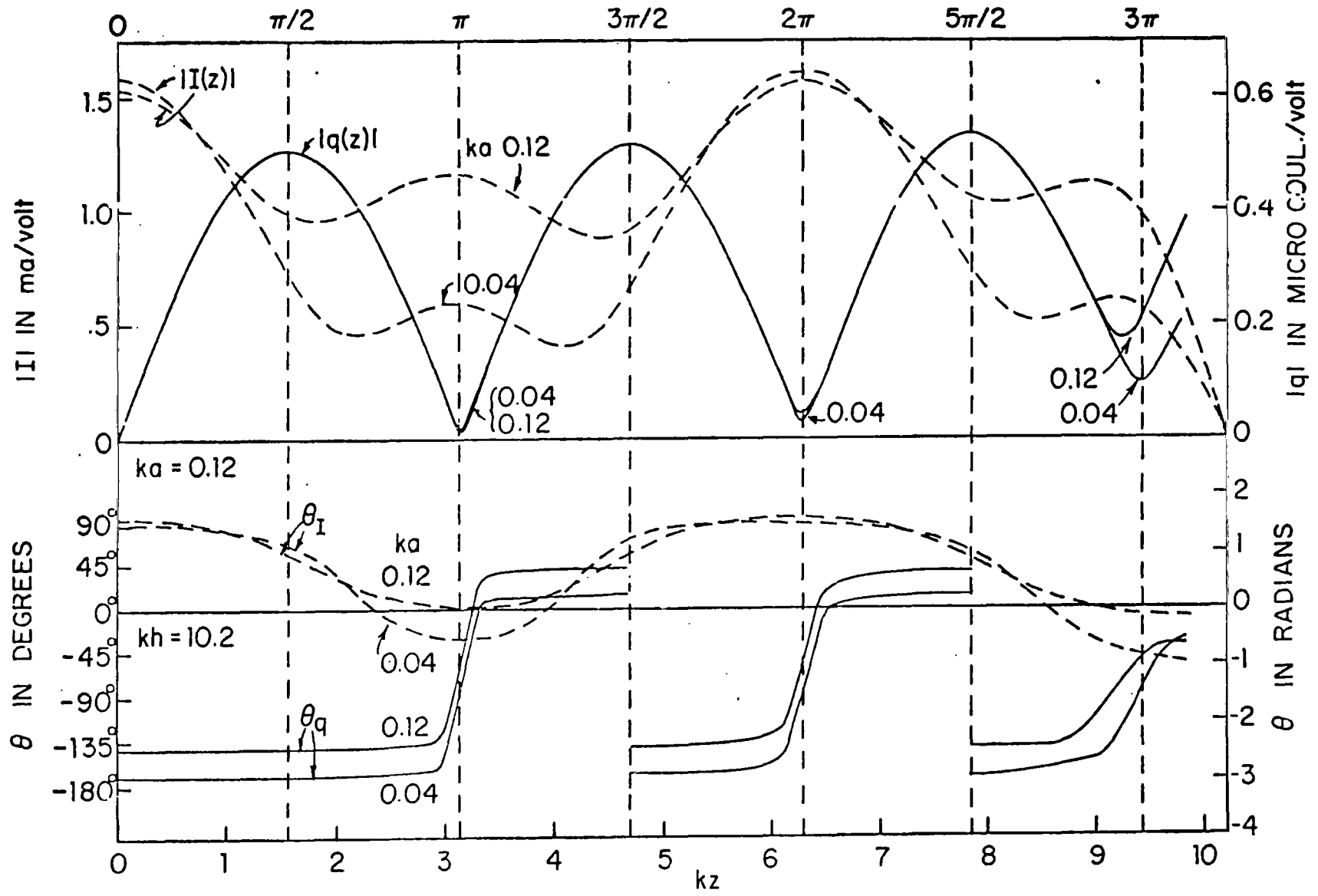

FIG. 7 THEORETICAL DISTRIBUTIONS OF CURRENT AND CHARGE PER UNIT LENGTH IN PARASITIC ANTENNA IN NORMALLY INCIDENT FIELD, h=1.62 λ

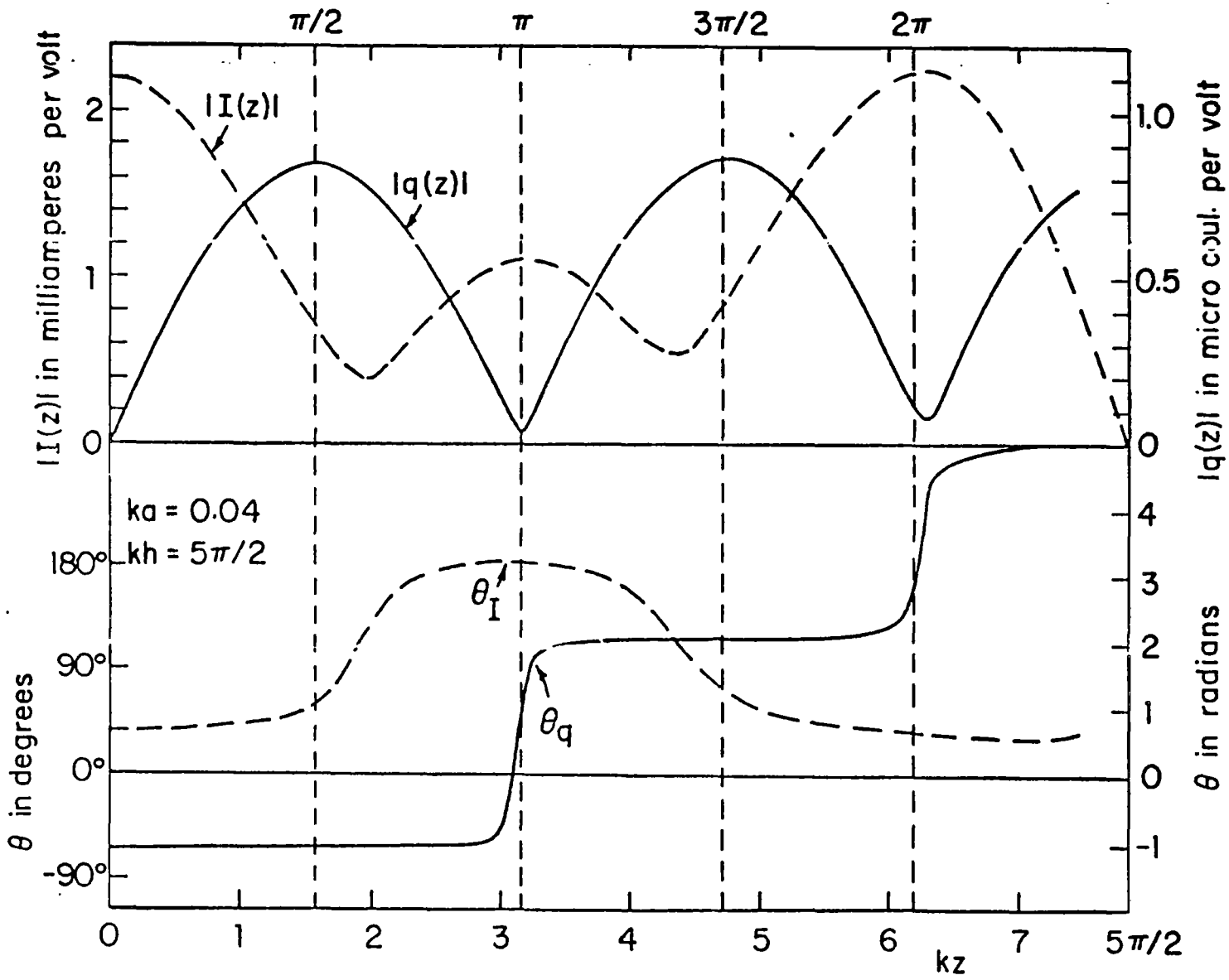

FIG. 8 THEORETICAL DISTRIBUTIONS OF CURRENT AND CHARGE PER UNIT LENGTH IN PARASITIC MONOPOLE IN NORMALLY INCIDENT FIELD, $h = 5\lambda/4$.

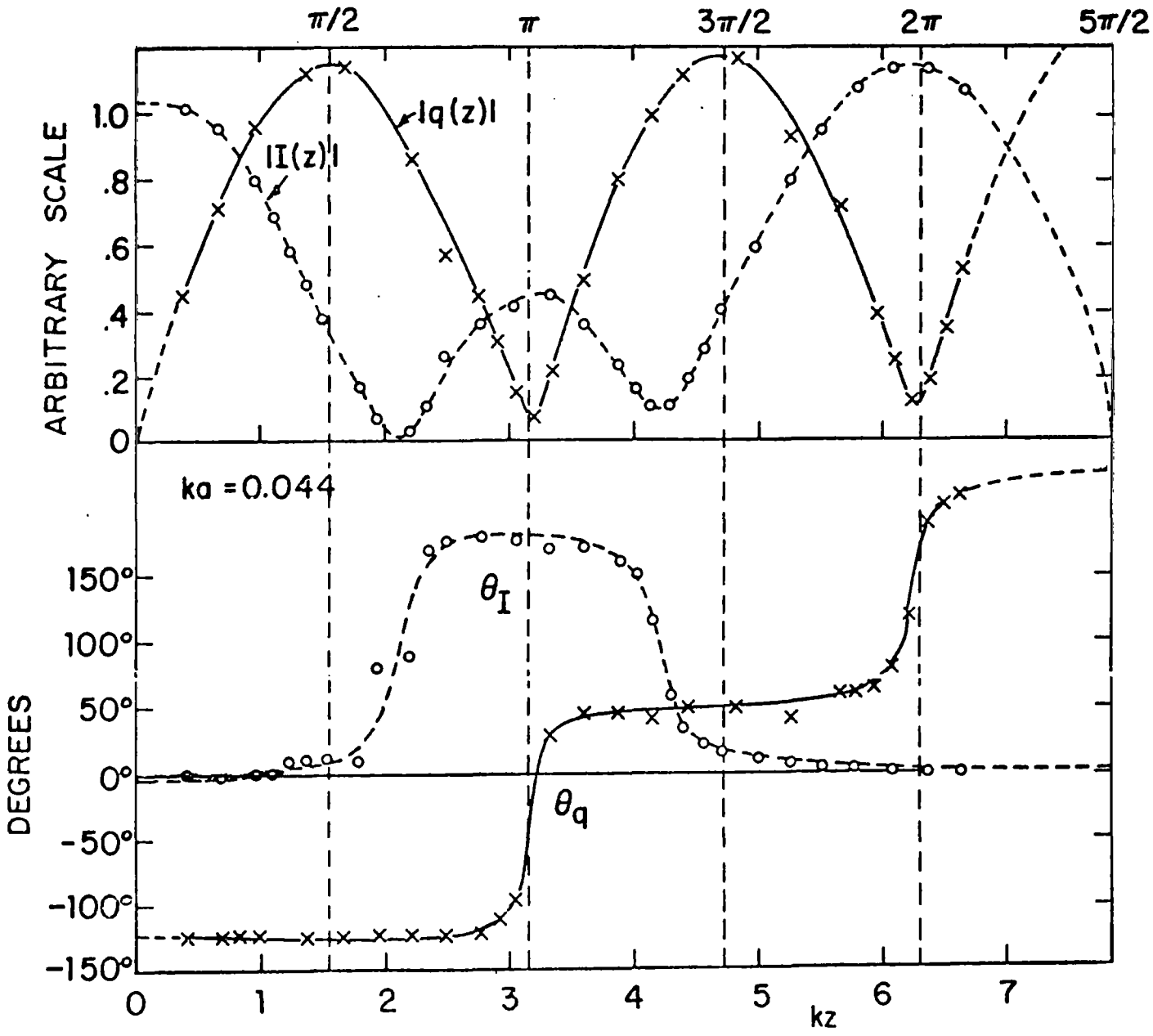

FIG. 9 MEASURED DISTRIBUTIONS OF CURRENT AND CHARGE PER UNIT LENGTH IN PARASITIC MONOPOLE $h = 5\lambda/4$

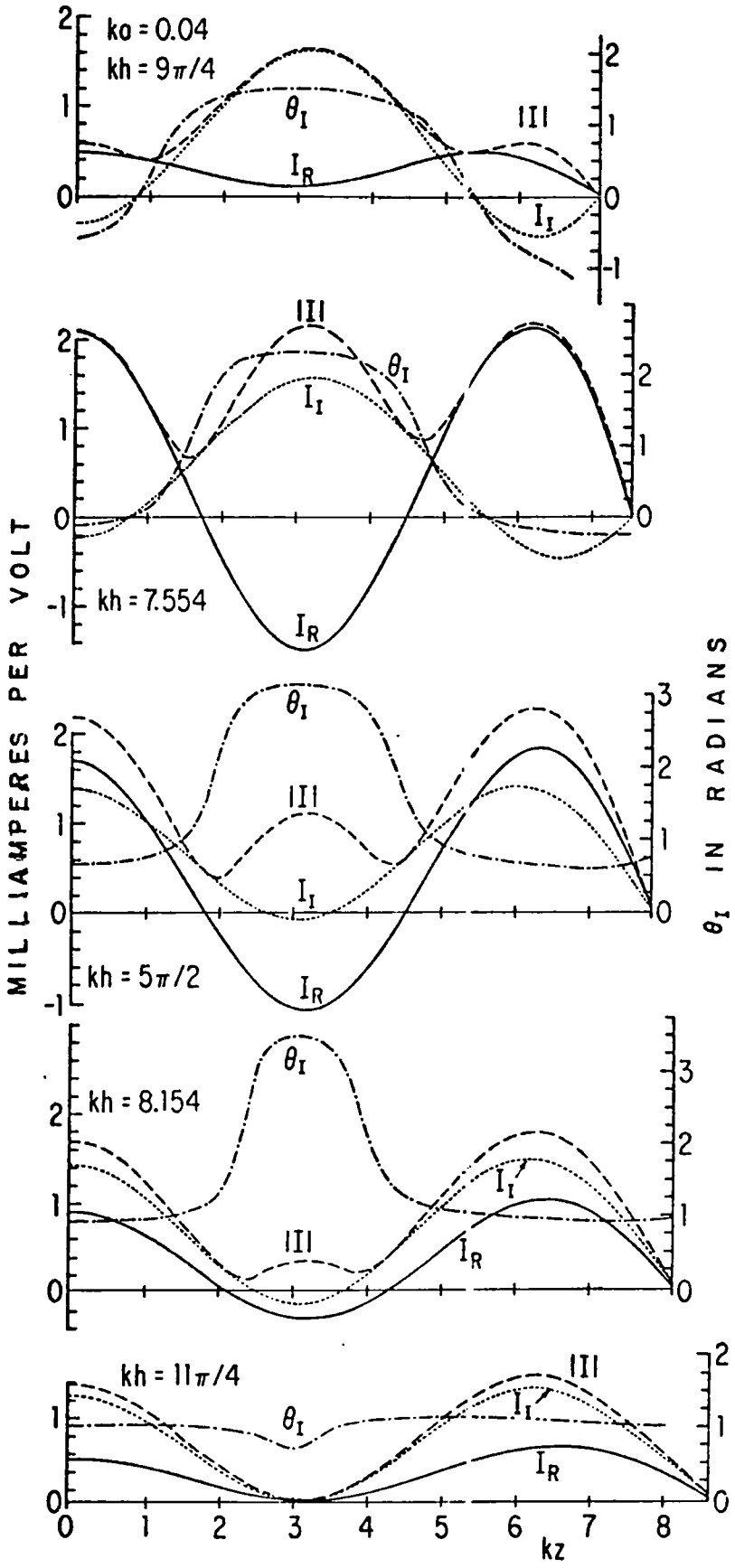

FIG. 10 THEORETICAL DISTRIBUTIONS OF CURRENT ON A PARASITIC MONOPOLE IN A NORMALLY INCIDENT FIELD.

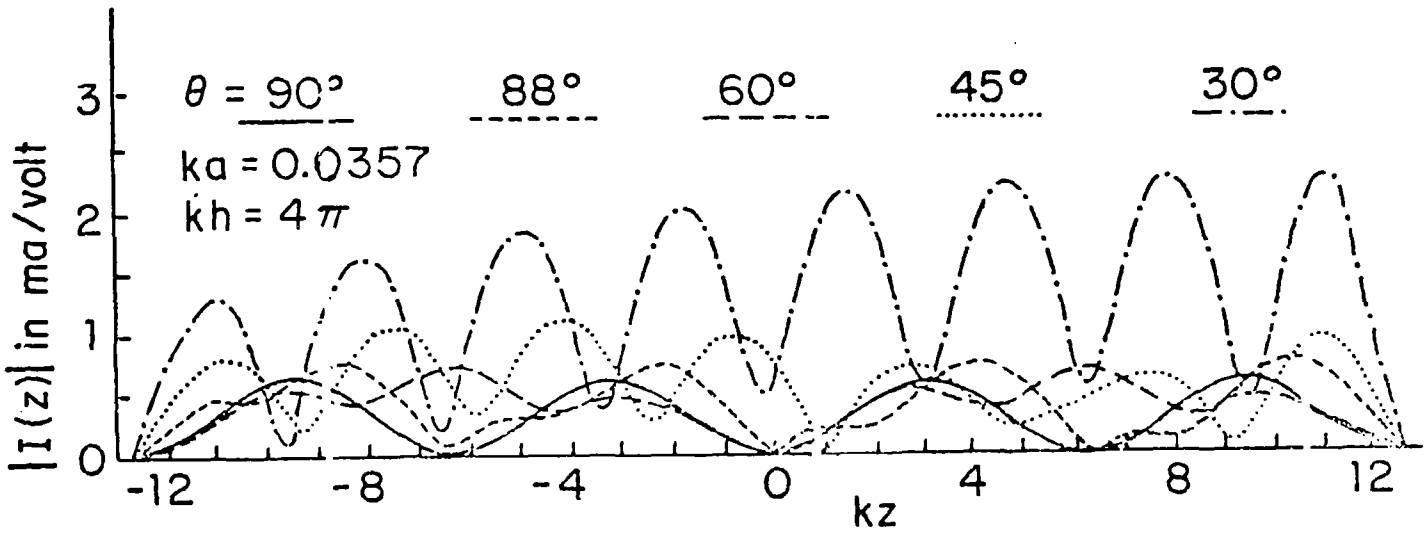

FIG. 11 INDUCED CURRENT IN PARASITIC ANTENNA; $\theta = 90°$ IS NORMAL INCIDENCE WITH E PARALLEL TO AXIS.